A drug delivery system based on poly-L-lysine grafted mesoporous silica nanoparticles for quercetin release

Cristina Carucci[1,2], Giulia Sechi,[1] Marco Piludu,[3] Maura Monduzzi,[1,2] Andrea Salis*[1,2]*

[1]*University of Cagliari, Department of Chemical and Geological Science, Cittadella Universitaria, 09042 Monserrato-Cagliari, Italy*

[2]*Consorzio Interuniversitario per lo Sviluppo dei Sistemi a Grande Interfase (CSGI), via della Lastruccia 3, 50019, Sesto Fiorentino (FI), Italy.*

[3]*Dipartimento di Scienze Biomediche, Università di Cagliari, Cittadella Universitaria, SS 554 Bivio Sestu, 09042 Monserrato, CA, Italy*

ABSTRACT

This work focuses on the preparation of a pH-sensitive antimicrobial drug delivery system based on Mesoporous silica nanoparticles (MSN), functionalized with aminopropyl-triethoxysilane (MSN-NH_2), triethylenetetramine (MSN-TETA) and poly-L-lysine (MSN-NH_2-PLL, MSN-TETA-PLL), and loaded with the flavonoid quercetin. The systems were fully characterized by means of several techniques. Besides the role of the different functionalization of MSNs, this work aimed to optimize both loading and release processes of quercetin, using two different ethanol-water mixtures as solvent, namely EtOH:H_2O mixtures at the ratios 80:20 and 50:50. Whereas loading was higher using the 80:20 solvent mixture, a more efficient release was ascertained using the solvent mixture 50:50 as demonstrated by the release kinetics, and also by the amount of the released drug. It was suggested that in the presence of less ethanol, quercetin solubility decreases, and a physical adsorption of quercetin at the functional groups of MSNs can be favoured with respect to a random distribution over many surface sites with which only weak interactions can occur. This means that in the presence of high amount of ethanol, used very often when dealing with poorly water-soluble drugs, the impregnation process becomes dominant, loading increases significantly, but subsequently burst release of high amounts of drug occurs. In this work, using the specific case of quercetin, we found a more sustained release as the result of a predominant adsorption mechanism due to the careful choice of the solvent mixture composition during the loading step. Moreover, the new drug delivery system allowed for a significant improvement in quercetin stability and the optimal release concentration attainment.

*Corresponding authors: Dr. Cristina Carucci cristina.carucci@unica.it, Prof. Andrea Salis asalis@unica.it

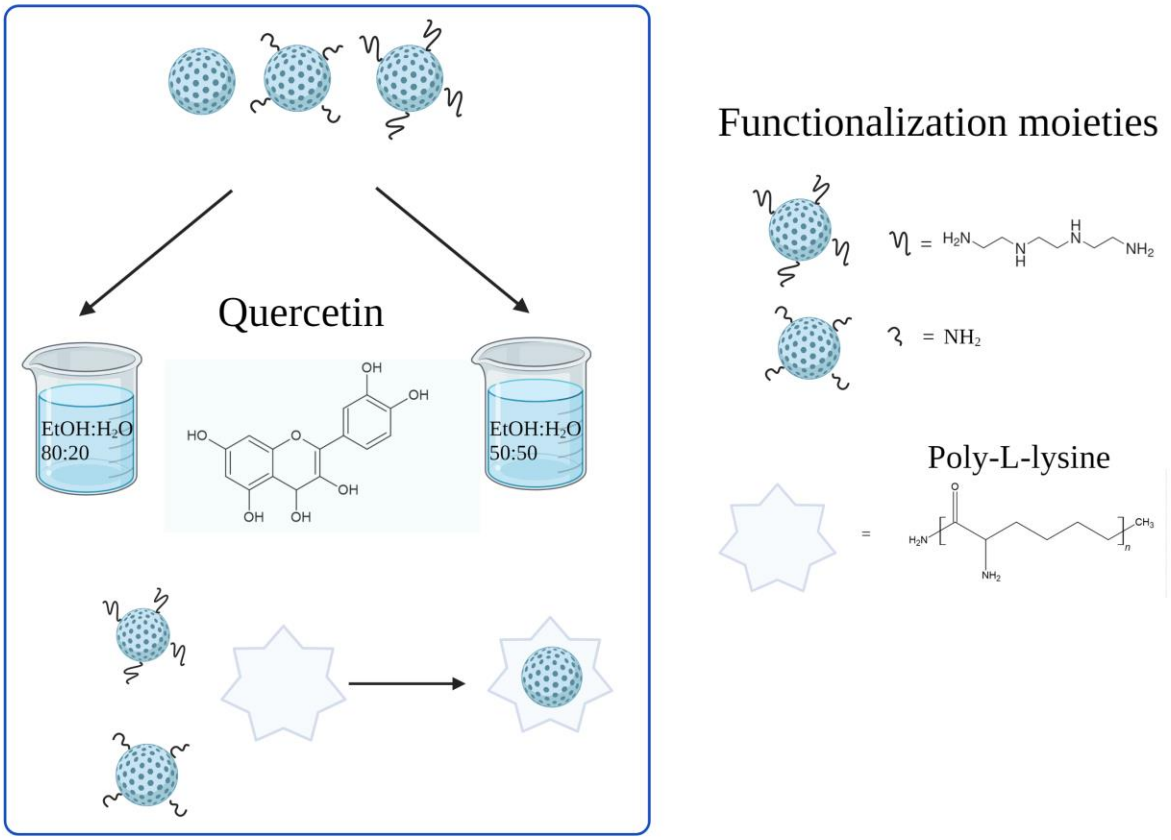

GRAPHICAL ABSTRACT: Quercetin loading with two EtOH:H_2O mixtures on MSN, MSN-NH_2, MSN-TETA. Functionalization on MSN-NH_2, MSN-TETA to obtain MSN-NH_2-PLL and MSN-TETA-PLL.

1. Introduction

The increasing demand of new drugs and smart drug delivery systems (DDS) to counteract antibiotic resistance has promoted wide-ranging research approaches to produce versatile and tunable DDS platforms, often based on hybrid multifunctional nanomaterials.[1,2] The choice of functionalized nanostructured drug carriers allows to protect and transport drugs to the desired target at the appropriate concentration.[3–5] Among a wide range of nanomaterials used to this purpose (i.e. polymeric micelles,[6] liposomes,[7] iron oxide nanoparticles[8]), significant advances have been achieved through the use of functionalized mesoporous silica nanoparticles (MSN) and antimicrobial agents such as flavonoids and polypeptides.[9,10] Indeed, mesoporous silica nanoparticles (MSN) are one of

the most promising nanocarriers thanks to their peculiar features, such as high surface area (up to 1000 m^2/g), narrow pore size distribution and easy surface functionalization.[11–15] Functionalization of MSNs plays a crucial role in addressing the diverse applications in nanomedicine, particularly the preparation of DDS. Several previous works have clearly demonstrated that surface functionalization are essential first of all to reduce cytotoxicity, that is affected by surface charge and size of MSNs. More specific functionalization may overcome other drawbacks that depend on several parameters, such as type of drug and biological target, loading and release features, administration route, bio-accumulation and bio-degradation of MSNs. [19,20] [19,20] For instance some specific functional groups can allow MSNs for oral drug administration,[5] others may prevent burst release when weak interactions between the nanoparticle surface and the drug occur.[16,18,21] Among polymers, cationic antimicrobial peptides (AMP) have been recognized to be very promising against multi-drug resistant bacteria and fungi.[1,2,5,22] Among diverse AMPs, poly-L-lysine (PLL), in addition to its potential as antimicrobial agent, characterized by low cytotoxicity, biocompatibility and biodegradability, provides stimuli responsive properties.[23] Indeed, due to pK_a around 9 of amino groups, PLL under physiological condition at pH ≈ 7, is positively charged.[24] Hence, PLL-grafted MSN have been studied as water soluble cationic pH responsive drug delivery systems.[25,26]

Quercetin (5,7,3,4'-hydroxyflavanol) is a flavanol found in a wide range of plants[27] and food products such as onions, berries, and cilantro.[28] Among its numerous properties such as anti-inflammatory,[29] antineoplastic[30] and antioxidant activity[31] quercetin has been recently evaluated for its antibacterial[32] and antiviral[33] uses. Quercetin antibacterial mechanism is due to destruction of plasma membrane and inhibition of bacteria's nucleic acid synthesis.[34,35] More recently free quercetin has been studied as a possible antibiotic alternative.[36] Unfortunately, quercetin shows low bioavailability and limited cellular absorption due to its low solubility in water.[37,38] In addition, quercetin suffers of severe photo- and thermo-sensitivity which makes it difficult to use for biomedical applications except when taken at high oral doses (200-500 mg three-five times a day).[38,39] Berlier et al. loaded quercetin on MSNs functionalized with octyl groups to study its topical use to prevent skin damage from light.[40] MSN-

NH_2 were also studied as carriers for topical quercetin delivery. Quercetin loaded MSNs have also been studied as a potential anti-cancer DDS, as in the work by Sarkar et al. which found that with folic acid induced apoptosis in breast cancer cells.[41] Loading quercetin on MSNs helped to overcome this issue for topical administration in the use of creams and ointments. Many other interesting cases of quercetin loaded on functionalized MSNs, [42–45] where mostly in vitro biological assays were used, can be cited. Several strategies to enhance the therapeutic effect of quercetin together with a wide range of loading approaches have been reported.[42,43,46,47] For example, Liang et al.[47] reported the use of ultrasound to increase quercetin loading on hollow zein chitosan coated nanoparticles in simulated gastrointestinal digestion conditions. Badens et al. studied the supercritical CO_2 impregnation method with ethanol 5 and 8% as cosolvent reaching up to 320 µg/g of quercetin in silica beads.[45] Khan et al.[43] loaded quercetin in diverse water ethanol mixtures ratio to obtain hollow-zein chitosan particles in a wide range of quercetin loading (from 100 to 200 µg/mL). Specifically, due to its low solubility, both impregnation and adsorption procedures have been studied to optimize quercetin loading on MSNs.[38,48–50] Sapino et al.[50] used the impregnation method dissolving quercetin in methanol for drug topical delivery. Zaharudin et al.[51] used pure ethanol as solvent and studied the effect of differently functionalized MSNs on quercetin loading and release. Ghanimati et al.[48] analyzed the adsorption of quercetin from water–ethanol (0-100%) mixtures achieving high drug loading values at basic pH. Rubini et al. compared the loading of quercetin on gelatin films by dissolution in either DMSO or EtOH:H_2O (50:50) mixtures.[49] Kazakova et al. found that increasing the EtOH content in a EtOH:H_2O mixtures increased quercetin solubility at the expense of quercetin adsorption on silica NPs.[52] In summary, most previous works have indicated strong associations between loading methods and the solvent mixtures used for quercetin loading to improve drug delivery systems design. However, the correlation between the solvent mixture used for quercetin loading and subsequent release has not exhaustively been investigated. Indeed, the effect of loading methods and solvent mixture composition was often investigated to maximize quercetin loading in carriers.[49–54] To the best of our

knowledge, the effect of the mixture composition used for quercetin loading on release rates from MSN have barely been considered.

Herein, the impact of the quercetin loading mixtures on release kinetic from MSN based drug delivery systems was studied. To this purpose, a DDS based on quercetin loaded on functionalized MSNs was prepared. MSNs were characterized through TEM, SAXS, FTIR, TGA, ELS and N_2 adsorption/desorption isotherms. Functionalization to introduce propyl-NH_2, TETA (triethylenetetramine) and PLL moieties, was performed. The effect of EtOH:H_2O mixture composition (80:20 and 50:50) on quercetin loading on MSNs, MSN-NH_2 and MSN-TETA was investigated. Then, quercetin release under physiological conditions for the DDS obtained from two EtOH:H_2O solvent ratios used in the loading step, was quantified along with the release dependence on functionalization moiety. Finally, the PLL grafted samples were investigated to evaluate quercetin stability together with the optimal release concentration.

2. Materials and methods

2.1 Reagents

Hexadecyltrimethylammonium bromide (CTAB > 99%), tetraethoxysilane (TEOS 98%), toluene (99.8%), 3-aminopropyl-triethoxysilane (APTES > 98%), triethylenetetramine (TETA ≥ 97%), NaH_2PO_4 (99%), Na_2HPO_4 (99%), NaCl, NaOH pellets, (3-chloropropyl)trimethoxysilane (CPTMS ≥ 97%), ammonium nitrate (NH_4NO_3 99%), HCl (37%), quercetin HPLC grade (≥ 95%), dimethylformamide (DMF ≥ 99,9%), aqueous glutaraldehyde (50%), poly-L-lysine hydrobromide (mol wt 15000-30000) were all purchased from Sigma Aldrich (Italy). Ethanol (99.8%) was purchased from Honeywell.

2.2 MSN synthesis and functionalization

MSN synthesis was carried out following a published protocol which provides MSN grafting prior CTAB removal.[13] (see details and physico-chemical characterization in Supporting Information).

2.3 Quercetin loading on bare and functionalized MSN

Quercetin loading was performed with two EtOH:H_2O mixtures at two different ratio. For mixture 80:20 EtOH:H_2O MSN, MSN-NH_2, MSN-TETA, MSN-NH_2-PLL and MSN-TETA-PLL were loaded by soaking 120 mg of each sample in 12 mL of a quercetin solution (10 mg/mL). For mixture 50:50 EtOH:H_2O, MSN, MSN-NH_2, MSN-TETA, MSN-NH_2-PLL and MSN-TETA-PLL were loaded by soaking 50 mg of MSN in 2 mL of a quercetin solution (2.5 mg/mL). All suspensions were stirred on a rotational shaker at 15°C for 24 h. All suspensions were then centrifugated and the supernatant removed. Materials were all dried under vacuum prior use. To determine drug loading on MSN, the supernatant concentration was determined by measuring the absorbance at 375 nm (final drug concentration) using the appropriate calibration curve (Fig. S2). Drug loading was calculated by the equation:

$$Drug\ loading(\frac{mg}{g}) = \frac{([D]_i - [D]_f)V}{m} \quad (1)$$

Where, $[D]_i$ and $[D]_f$ are the initial and final drug concentrations (mg/mL), respectively. V is the volume of drug solution (mL) and m is the mass of the MSN carrier (g).

2.4 Kinetics of quercetin release

To study quercetin release, a mass of 50 mg of quercetin loaded sample were dispersed in 50 mL of phosphate buffer saline (PBS) 100 mM, NaCl 150 mM at pH 7.4. Each sample was stirred (156 rpm) and incubated at 37°C. After 1 h, 2 h, 3 h, 4 h, 5 h, 6 h and then after 24 and 25 h, 3.5 mL of sample were collected and immediately replaced with the same volume of fresh PBS solution to maintain *sink conditions*.[55] The amount of drug released was determined at wavelength of 375 nm. The same measurement was performed at pH 3 and pH 7.4 for MSN-NH_2-PLL and MSN-TETA-PLL. The acidic conditions were chosen to assess MSN-PLL responsiveness in comparison with the physiological pH 7.4. At pH 3 Indeed, at pH 3 the amino groups of PLL are fully ionized thus the formation of a shrunken form α-helical structure is prevented[56] whereas a random elongated coil

shape occurs that, in turns, favors the opening of the pores.[57] PBS was used at both pH to avoid the use of a different buffer as reported for MSN-PLL gatekeeper.[57]

$$Drug\ \ concentration(\frac{\mu g}{mL}) = A_{max}(1 - e^{-k_1 t}) \quad (2)$$

The quantity of released quercetin has been calculated according to equation 2, where drug concentration represents the amount of drug released at specific time (μg/mL), A_{max} is the maximal concentration of released drug (μg/mL) and k_1 (h^{-1}) is the release constant rate

2.5 Quercetin stability

Quercetin at concentration 2 μg/mL were dissolved in PBS buffer 100 mM, NaCl 150 mM, at 37°C at pH 3 or at pH 7.4. Immediately after preparation, after 6 h and 24 h of incubation 3.5 mL of sample were withdrawn and UV-vis spectra were registered from 200 to 800 nm. Release spectra of quercetin from MSN-NH_2, MSN-TETA, MSN-NH_2-PLL and MSN-TETA-PLL were registered in the same wavelength range after incubation in the same conditions.

3. Results and discussion

3.1 Characterization of MSN, MSN-NH_2 and MSN-TETA

Synthesized MSNs were characterized by TEM, SAXS and N_2-adsorption techniques. TEM images in Fig. 1 (A-B) show MSNs particles having ellipsoidal shapes with an internal structure constituted by typical parallel channels. SAXS pattern of MSNs in Fig. 1C displays an intense peak relative to the reflection of the 100 plane and three less intense peaks due to 110, 200 and 210 planes. This pattern confirms the occurrence of an ordered 2D hexagonal phase with a lattice parameter a = 47 Å. The functionalization of the external surface of MSNs of propyl-NH_2 and TETA moieties to obtain MSN-NH_2 and MSN-TETA samples, respectively, was carried out before CTAB extraction as previously reported.[58] MSN were characterized by FTIR spectroscopy. All samples show the characteristic peaks around 1060 cm^{-1} and 800 cm^{-1} due to the stretching vibrations of Si-O-Si bond (Fig. S1). Successful post functionalization CTAB extraction was confirmed by the disappearance of

C-H stretching bands at 2922 cm^{-1} and 2853 cm^{-1}. MSN-CTAB-NH_2 and MSN-NH_2 spectra show -NH_2 bending at 1560 cm^{-1}. To obtain MSN-TETA sample, the grafting of the propyl-Cl moiety is needed as first step leading to the synthesis of MSN-CTAB-Cl. MSN-CTAB-Cl synthesis is confirmed by the clear disappearance of silanol peak at 970 cm^{-1}. The so functionalized MSN was then treated with TETA. MSN-CTAB-TETA and MSN-TETA spectra show a band at 1654 cm^{-1} due to the NH_2 bending (Fig. S1). The structural order typical of MCM-41 materials[59] is retained after propyl-NH_2 and TETA functionalization as confirmed by the SAXS patterns showing the hexagonal phase (Fig. 1C) and the unaltered lattice parameter values (Table 1). MSN sample has a BET surface area of 1142 m^2/g which decreases for MSN-NH_2 and MSN-TETA sample to 630.3 and 717.2 m^2/g, respectively. A slight decrease of pore size from 2.8 nm (MSN) to 2.5 nm (MSN-NH_2) and 2.3 nm (MSN-TETA) is shown. While there is not functionalization present within the pores, surface area and pore size decrease could be due to a partial closure of pore openings consequent to the external functionalization on MSN surface.

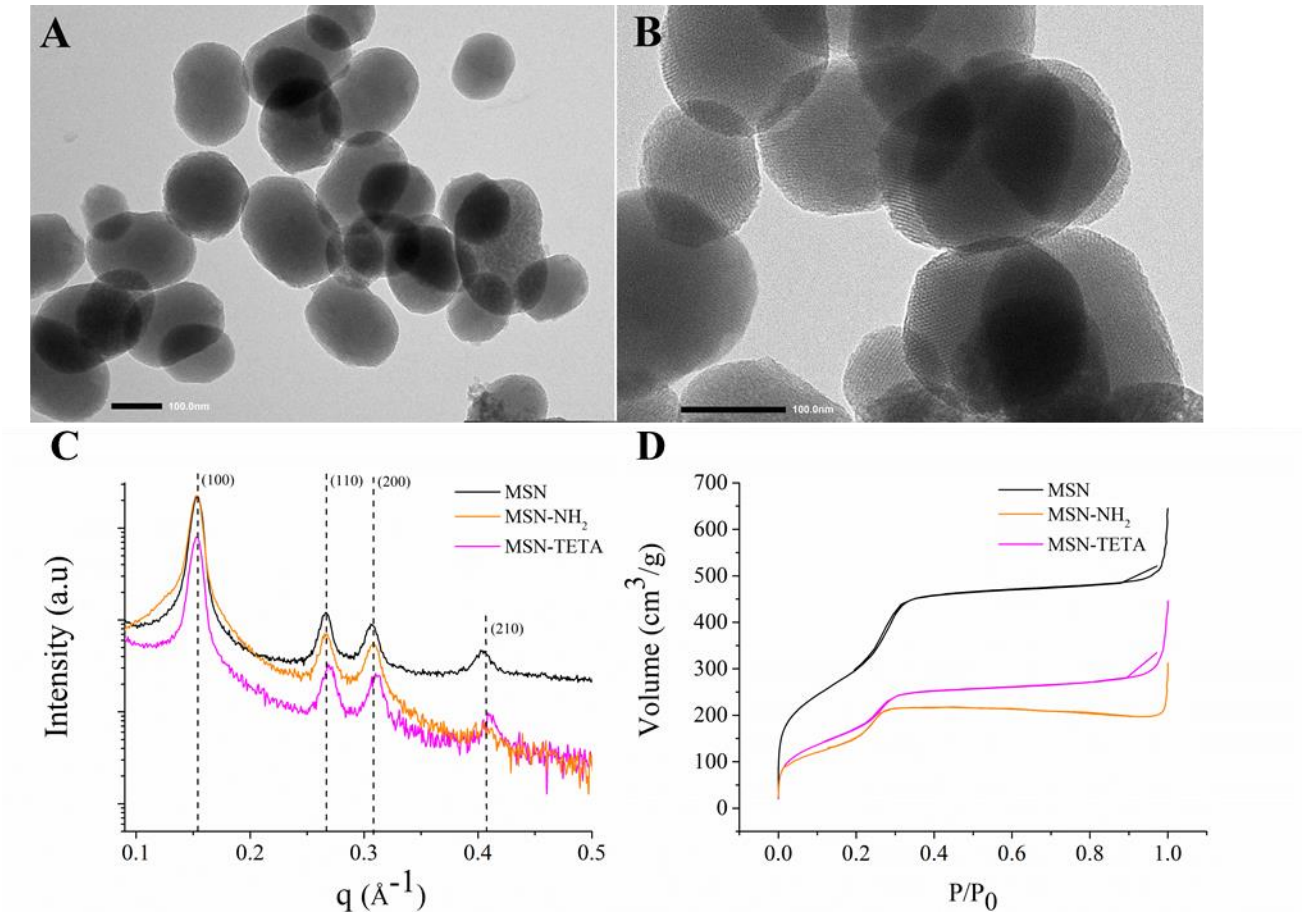

Figure 1. TEM images of MSN at different magnifications A-B) structural characterization of MSN, MSN-NH_2 and MSN-TETA as C) SAXS patterns D) adsorption/desorption N_2 isotherm.

Table 1. Samples characterization data.

Sample	[a]S_{BET}(m^2/g)	[b]V_P (cm^3/g)	[c]d_P (Å)	[d]*a* (Å)
MSN	1142	0.9	28	47
MSN-NH_2	630	0.4	25	47
MSN-TETA	717	0.6	23	47

[a] Surface area calculated by BET method, pore volume from the desorption branch calculated at P/P_0=0.99 by BJH method, [b] pore volume and [c] pore diameter calculated with BJH method to the isotherm desorption branch, [d] lattice spacing of MSNs calculated with the equation $a_{(hex\ phase)} = (2/3^{0.5})\times(h^2 + k^2 + l^2)^{0.5}$.

To confirm nanoparticles functionalization, TG analysis of MSN in comparison with MSN-NH_2 and MSN-TETA samples was performed (Fig. 2). Mass losses < 100° C are attributed to the loss of humidity. In the temperature range between 100 °C and 250 °C a mass loss of 12.1% and 7.9% attributed to the organic moieties of MSN-NH_2 and MSN-TETA, respectively. The mass losses for MSN-NH_2 and MSN-TETA at 250°C are likely due to the sole MSN external functionalization. This might provoke a net loss of the propyl-NH_2 and triethylenetetramine moiety which causes a sudden

drop in mass. These mass losses correspond to an amount of grafted functional group of 110.8 mg/g for MSN-NH_2 and of 76.8 mg/g for MSN-TETA (Table 2). PLL modification is confirmed by TG analysis in the range of temperature 250-575 °C with a mass loss of 20 % and 27.4% for MSN-NH_2 and MSN-TETA, respectively, as shown in Figure 2.

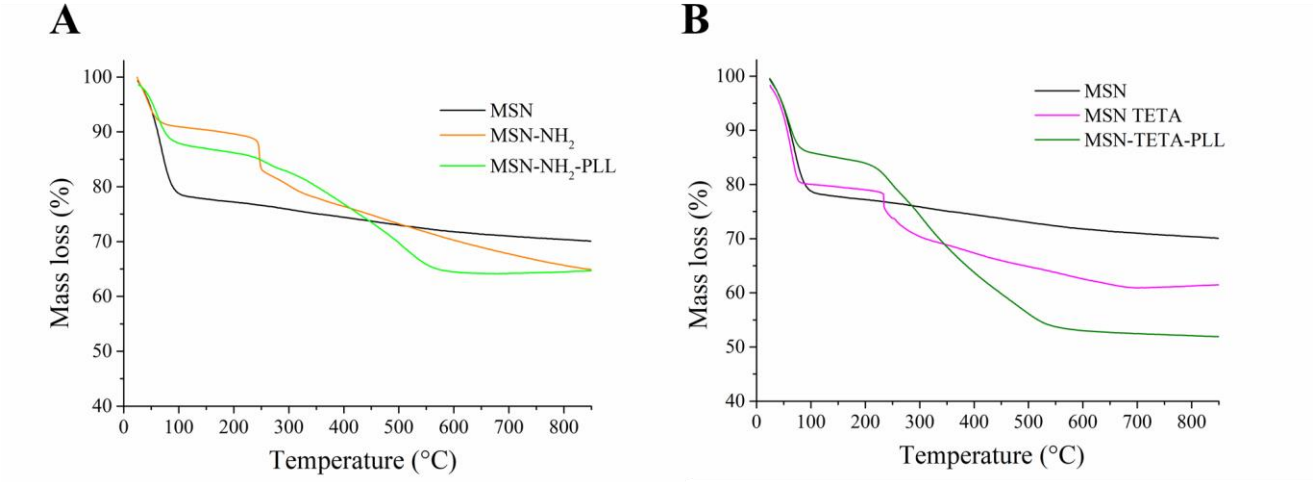

Figure 2. Thermogravimetric analysis of A) MSN, MSN-NH_2, MSN-NH_2-PLL and B) MSN, MSN-TETA, MSN-TETA-PLL.

Table 2. Mass losses % and amount of grafted functional groups (mg of moiety per g of MSN) calculated from TGA data for functionalized MSN samples. Isoelectric point (pI) from zeta potential measurements (Fig. 4)

Sample	25 °C < T< 100 °C	100 °C < T < 250 °C	250 °C < T< 575 °C	Func. moiety (mg/g)	pI
MSN	21.6	-	-	-	4.2
MSN-NH_2	8.8	12.1	10.0	110.8	7.9
MSN-NH_2-PLL	13.1	2.5	20.0	100.3	8.3
MSN-TETA	20.2	7.9	13.4	76.8	9.1
MSN-TETA-PLL	15.5	6.7	27.4	140.7	9.8

3.2 Quercetin loading and release from MSN, MSN-NH_2, MSN-TETA

Drug loading on MSNs can be obtained by impregnation or adsorption methods or a combination of both. In the former, a solvent where the drug is highly soluble is used. The solvent must also have a

low surface tension, so that it can easily evaporate leaving the drug inside the mesopores. In the latter, the drug should not have a high solubility in the solvent, otherwise the establishment of attractive interactions with the particles' surface would be unfavored. Sometimes both impregnation and adsorption phenomena are simultaneously at work. Although the effect of the solvent on drug loading is usually considered, the successive effect on the release has not been deeply investigated yet. The highest quercetin loadings are usually achieved when using pure ethanol.[48] However, drug distribution after impregnation is difficult to control.[60] For example, Popova et al. used the impregnation method by dissolving quercetin in pure ethanol.[61] They obtained a burst release (60% of drug mass in 30 mins) from bare silica particles, likely because of the lack of attractive interactions between quercetin and the silica surface. Enhancements in drug loadings were studied with a variety of drugs. For example, Paclitaxel loading on MSN was assessed in three different solvents, specifically dichloromethane, ethanol and DMSO. In that work, the highest loading was found with drug dissolution in dichloromethane. However, the drug release study was performed after drug loading on this solvent only with a cumulative drug release of 34.4% after 48 h.[44]

In our case quercetin loading on MSNs was firstly carried out dissolving the drug in a mixture of EtOH:H_2O 80:20 (v/v). This solvent mixture result in a quercetin loading, quantified by UV-Vis analysis, corresponding to 627.6 mg/g for bare MSNs, and 98.2 mg/g for MSN-NH_2 and 347.6 mg/g for MSN-TETA (Table 3). A mixture of EtOH:H_2O 50:50 (v/v) was also used to load quercetin. The lower ethanol content in the solvent mixture resulted in a lower quercetin loading for all samples, with the highest obtained for MSN-TETA (92.8 mg/g) and MSN-NH_2 (92.6 mg/g) and the lowest for bare MSNs (80.4 mg/g). The higher quercetin loading obtained for EtOH:H_2O 80:20 mixture is consistent with a process in which impregnation prevails on adsorption. This result is also in agreement with what reported in the literature.[52]

Table 3. Effect of solvent mixture composition (EtOH:H_2O 80:20 and EtOH:H_2O 50:50) on quercetin loading and release (kinetic parameters: A_{max}, k_1 and R^2 calculated by fitting equation 2) from different MSN samples.

	EtOH:H_2O (80:20)				EtOH:H_2O (50:50)			
Release pH 7.4	**Loading (mg/g)**	**A_{max} (µg/mL)**	**k_1 (h^{-1})**	**R^2**	**Loading (mg/g)**	**A_{max} (µg/mL)**	**k_1 (h^{-1})**	**R^2**
MSN	627.6	1.8	80.9	0.93	80.4	3.8	1.3	0.96
MSN-NH_2	98.2	1.8	1.6	0.96	92.6	2.8	0.2	0.90
MSN-TETA	347.6	2.8	2.7	0.98	92.8	5.2	0.1	0.96

The effect of EtOH:H_2O ratio in the loading step on quercetin release was then studied. For samples loaded using 80:20 EtOH:H_2O ratio, the maximal concentration of released quercetin $A_{max,}$ was 1.8 µg/mL for MSN and MSN-NH_2 increasing up to 2.8 µg/mL for MSN-TETA. The release kinetic constant, k_1, was very high for bare MSN (80.9 h^{-1}) suggesting a burst release of quercetin. Lower values of k_1, 2.7 h^{-1} and 1.6 h^{-1}, were obtained for MSN-TETA and MSN-NH_2, respectively. This suggests the occurrence of attractive interactions between quercetin and the functionalized MSNs which slowed down the process making the release more sustained. Although, bare MSNs reached the highest quercetin loading with a solvent composition EtOH:H_2O 80:20, their release performance were very poor both in terms of A_{max} and k_1.

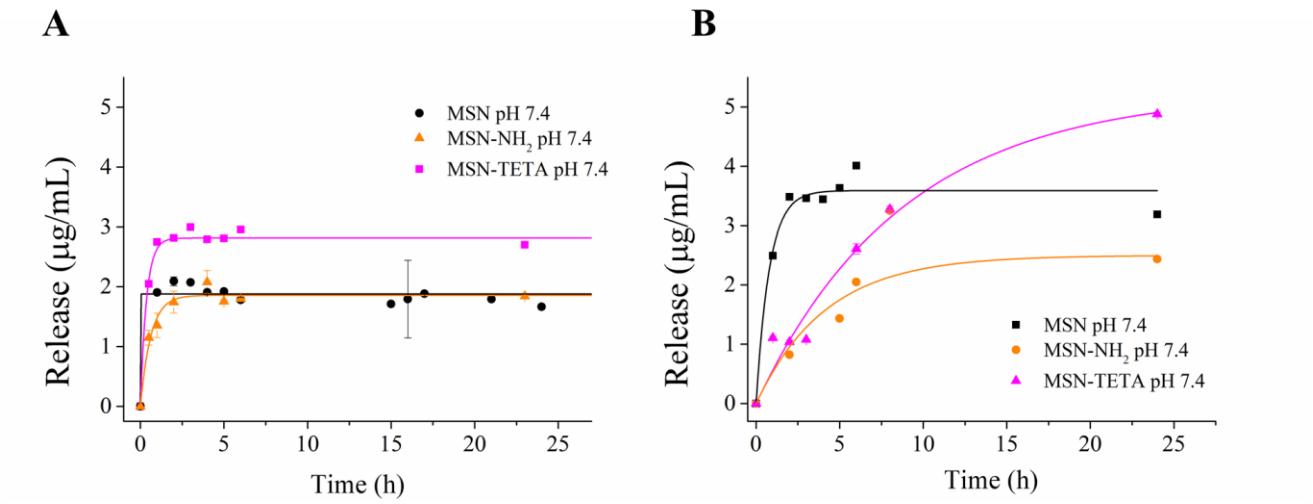

Figure 3. Quercetin release of MSN, MSN-NH_2, MSN-TETA after quercetin loading in a EtOH:H_2O mixture A) 80:20 and B) 50:50.

The use of a solvent composition (EtOH:H_2O 50:50) had the important effect to slow down the quercetin release and to modulate the maximal concentration of quercetin for all MSN samples. Bare MSN showed a fast quercetin release (k_1=1.3 h^{-1}) which was in any case much lower than that obtained for the 80:20 EtOH:H_2O mixture. In addition, both functionalized samples showed much slower release with values of 0.2 h^{-1} and 0.1 h^{-1} for MSN-NH_2 and MSN-TETA, respectively. Considering that quercetin is highly soluble in ethanol, but not in water, lowering ethanol content favors the physical adsorption on functionalized MSNs with respect to the impregnation process. The attractive interactions between the physically adsorbed drug at the functionalized silica surface slows down the release as demonstrated by the significant decrease of the kinetic constants reported in Table 3. The effect is clearly seen also in Figure 3B where almost no burst release occurs from both MSN-NH_2 and MSN-TETA matrices when the 50:50 EtOH:H_2O mixture is used. The decrease of release kinetic constants follows the order of MSN > MSN-NH_2 > MSN-TETA correlating the occurrence of a more sustained release with surface functionalization and indicating a general better performance of the DDS loaded with a lower ethanol content. $A_{max,}$ was 2.8 µg/mL for MSN and 3.8 µg/mL MSN-NH_2 with MSN-TETA showing the highest A_{max} at 5.2 µg/mL. These results suggest that adsorption is more useful than impregnation as a method to load quercetin on functionalized MSN carriers. Due to the better release performance of samples loaded with EtOH:H_2O 50:50 ratio, this solvent composition was chosen to study quercetin loading and release from PLL-grafted MSN samples.

3.3 PLL grafting of MSN-NH_2 and MSN-TETA

It has often been reported that positively charged silica surfaces greatly reduce citotoxicity.[20,62–65] To this purpose we used the polypeptide PLL that, grafted to MSNs surface, besides providing a positive charge, is known to act as antimicrobial agent[1,2,5,22] and, more importantly, introduces stimuli responsive properties, being very sensitive to pH.[23] PLL was grafted to MSN-NH_2 and MSN-TETA by mean of glutaraldehyde. To confirm PLL grafting TG analysis of MSN-PLL in comparison with MSN, MSN-NH_2 and MSN-TETA samples was performed. (see Fig. 2 and Table 2). In the

temperature range 250°C - 700 °C, MSN-NH_2-PLL and MSN-TETA-PLL samples have mass losses of 20% and 27.4%, respectively, attributed to the combustion of PLL polymer. These values correspond to an amount of grafted PLL of 140.7 mg/g for MSN-TETA-PLL and of 100.3 mg/g for MSN-NH_2-PLL.

To further confirm PLL functionalization, zeta potential (ζ) of bare, functionalized, and PLL-grafted MSNs were measured as a function of pH (Figure 4). MSN showed an isoelectric point (pI) = 4.1 while for MSN-NH_2 and for MSN-TETA it increased to pI = 8.0 and 9.2, respectively. The pI of amino functionalized MSNs occurs at a higher pH value because of the presence of positively charged amino groups. MSN-NH_2-PLL and MSN-TETA-PLL show a further increase of the isoelectric point (pI = 8.3 and 9.8, respectively) thus confirming PLL functionalization (Table 2)

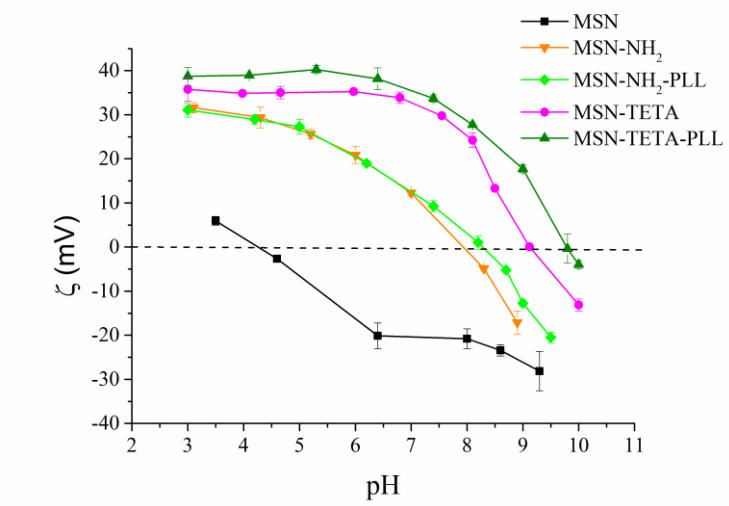

Figure 4. Zeta potential (ζ) as a function of pH in water for MSN, MSN-TETA, MSN-TETA- PLL, MSN-NH_2, and MSN-NH_2-PLL samples.

3.4 Quercetin loading and release from MSN-NH_2-PLL, MSN-TETA-PLL as function of pH

The obtained PLL-grafted MSN samples were then loaded with quercetin from a EtOH:H_2O 50:50 mixture. Quercetin loadings were 113.8 and 109.2 mg/g for MSN-NH_2-PLL and MSN-TETA-PLL, respectively. These values were slightly higher than those obtained for MSN-NH_2 (92.6 mg/g) and MSN-TETA (92.8 mg/g), likely due to the establishment of favorable interactions between quercetin and PLL chains. PLL is a pH responsive polymer that should change conformation going from neutral

to acidic pH.[24,57] To evaluate the pH response of the DDS, the release of quercetin from MSN-NH_2-PLL and MSN-TETA-PLL was carried out at two different pH values, namely, pH = 7.4 and 3 in PBS buffer.

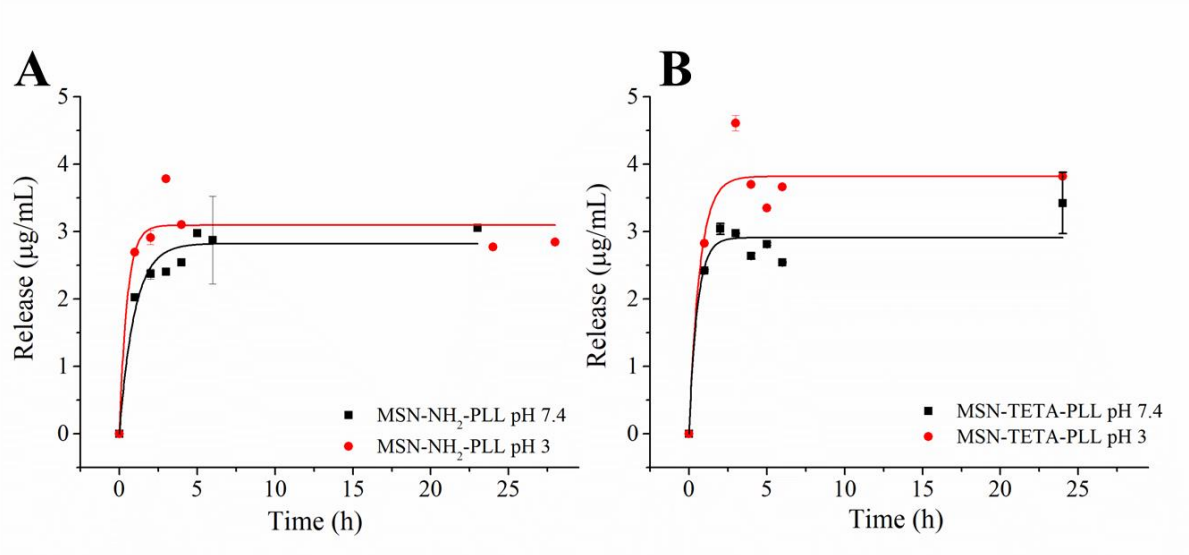

Figure 5. Quercetin release of A) MSN-NH_2-PLL and B) MSN-TETA-PLL at pH 3 and 7.4.

A change of pH should affect the maximal amount of released quercetin (A_{max}) because, in response to acidic pH, a conformation change of PLL should favor drug release.[66] However, in agreement with the slight change of zeta potential observed at pH 7.4 and 3, MSN-NH_2-PLL did not show a significant difference in pH response. Indeed, at pH 3 A_{max} = 2.6 µg/mL and 2.9 µg/mL at pH 7.4. Consistently with the change of zeta potential with pH, MSN-TETA-PLL was more sensitive to pH changes, resulting in A_{max} = 3.6 µg/mL and 2.8 µg/mL at pH = 3 and 7.4, respectively.[57]

Besides A_{max}, pH affects also k_1. Kinetic constants of quercetin release from MSN-NH_2-PLL decreases with decreasing pH from 2.6 h^{-1} at pH 7.4 to 1.3 h^{-1} at pH 3. Similarly, for MSN-TETA-PLL the kinetic constant decreases from pH 7.4 (1.7 h^{-1}) to pH 3 (1.5 h^{-1}). The decrease of k_1 suggests that quercetin interacts more strongly with PLL groups at acidic pH with a resulting slowdown of the release process. Quercetin molecule has 5 phenolic groups each having a different pK_a value (Table S1).[67,68] The first pK_a of quercetin measured by spectrophotometry is 6.74.[69] According to Diduk et al.[70] quercetin is only partially deprotonated at physiological pH 7.4.

At pH 7.4, the kinetic constants of both MSN-NH_2-PLL and MSN-TETA-PLL (2.9 and 2.8 h^{-1} respectively) are 15 times higher than the values found for MSN-NH_2 and MSN-TETA loaded at EtOH:H_2O 50:50 ratio (0.2 and 0.1 h^{-1} respectively) (Table 4). The higher k_1 values obtained for PLL-grafted samples might be due to quercetin adsorption mainly on the external surface rather than within mesopores. Quercetin loading was performed post-functionalization due to experimental constraints. If drug loading is carried out before -NH_2, -TETA or -PLL functionalization, it could cause an unwanted drug leaching during the following functionalization step. For this reason, the post functionalization loading is widely used.[71-73]Although we expect that a certain amount of the drug reaches the MSN pores after the PLL functionalization, we cannot exclude that part of the drug is adsorbed on PLL external surface.

Table 4. Kinetic parameters release for MSN-NH_2-PLL and MSN-TETA-PLL at pH 3 and 7.4.

	MSN-NH_2-PLL				**MSN-TETA-PLL**			
	Loading (mg/g)	**A_{max} (µg/mL)**	**k_1 (h^{-1})**	**R^2**	**Loading (mg/g)**	**A_{max} (µg/mL)**	**k_1 (h^{-1})**	**R^2**
pH 7.4	113.8	2.9	2.6	0.99	109.2	2.8	1.8	0.99
pH 3	113.8	2.6	1.3	0.98	109.2	3.6	1.5	0.99

A successful DDS should release an amount of drug that matches drug concentration in plasma within a therapeutic window.[74,75] Kaushik et al. studied quercetin concentration in plasma after oral administration of quercetin aglycone using various food supplements such as quercetin fortified bars and chews.[76] Quercetin concentration in plasma ranged from 0.2 to 3 µg/mL.[76] It is noteworthy that for PLL grafted MSN samples in the present work, the maximal concentration of released quercetin matches the concentration of quercetin in plasma after oral administration.

3.5 Quercetin stability

Quercetin shows low chemical stability depending on pH.[77–80] For example Lei. et al.[79] studied quercetin degradation at basic pH with electrogenerated chemiluminescence. Zenchevich et al.[80] studied quercetin at basic and acidic pH through UV-Vis spectroscopy and HPLC to analyze quercetin oxidation products. In our work the stability of free quercetin (at a concentration of 2 μg/mL) in PBS was studied by means of UV-Vis spectroscopy. The UV-Vis spectrum of quercetin at pH 3 displays two main peaks at 255 and 370 nm with no substantial change as a function of time (Fig. 6A). The spectrum of a freshly prepared sample of quercetin at pH 7.4 is slightly different from that at pH 3, showing two main peaks at 255 nm and 375 nm and one small peak at 316 nm, consistently with what reported in literature.[81] However, after 6 h of incubation under physiological conditions (T = 37°C and pH 7.4), quercetin solution showed a hypochromic shift. This band shift suggests a chemical change likely due to a loss of conjugation in slightly basic pH, as reported in literature.[82–86] More specifically at neutral and slightly basic pH values quercetin is rapidly oxidized.[87] It has been found that at alkaline conditions, the γ-pyrone fragment of quercetin decomposes with the formation of one isomer of a benzenetriol together with 2,4,6 trihydrobenzoic and 3,4 dihydroxybenzoic acid.[68,80] Fig.6 shows the UV-Vis of quercetin after release from PLL-grafted MSNs at different release times. At t = 6 h the UV-Vis spectrum of quercetin is exactly the same of that of the original molecule. According with UV-Vis spectra in Fig. 6D, quercetin is oxidized only after 24 h from the release by MSN-TETA-PLL at pH 7.4 and 37°C, thus indicating an improved storage stability of the drug immobilized on functionalized MSNs.

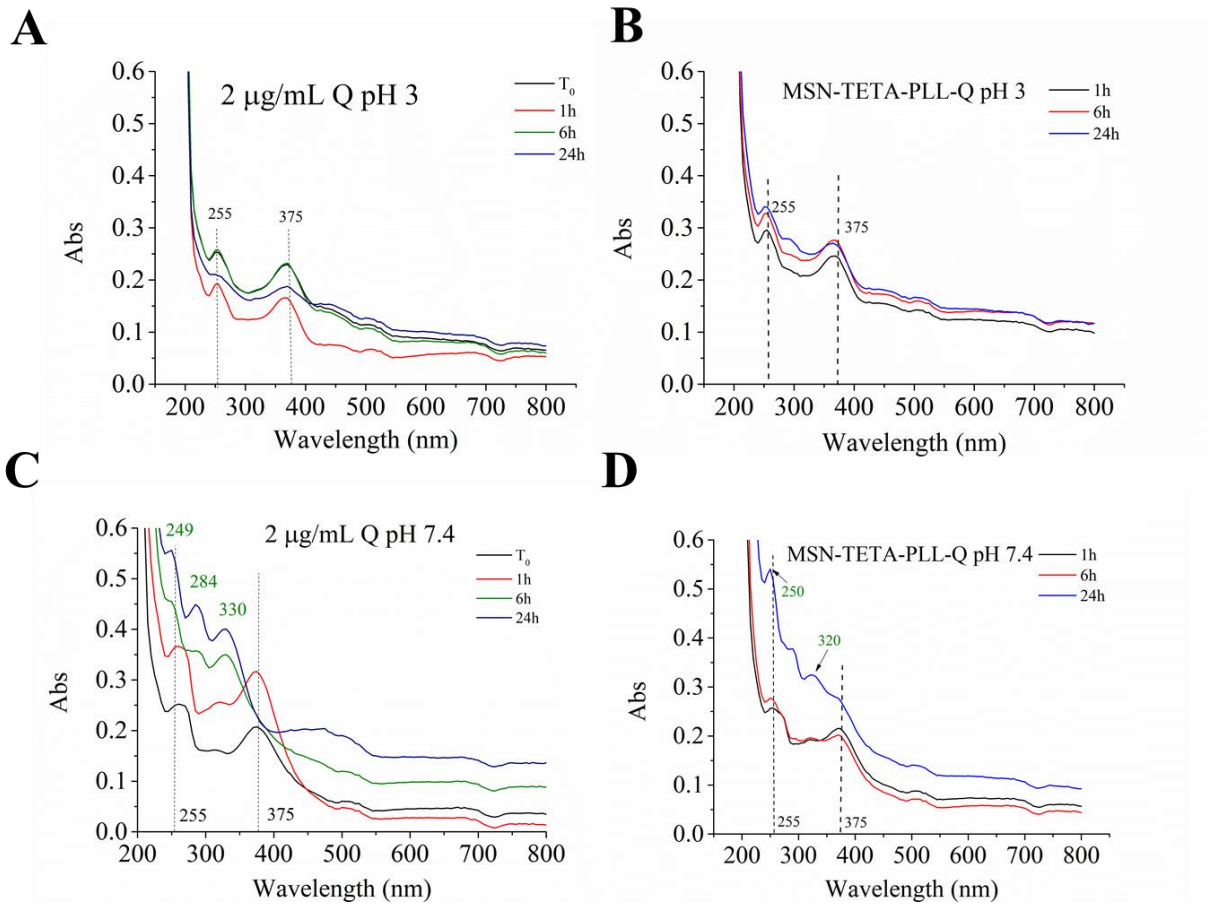

Figure 6. UV-Vis spectra of free quercetin at pH 3 A) and pH 7.4 spectra are reported as stack peaks to evaluate before (black values) and after degradation (green values) C) UV-Vis spectra of release quercetin solution from MSN-TETA-PLL pH 3 B) and pH 7.4 D) measured after different incubation times in PBS at 37 °C.

All functionalized samples, MSN-NH_2, MSN-TETA, MSN-NH_2-PLL (Fig. S3-S4) and MSN-TETA-PLL, have the same protective action toward quercetin molecule, thus they could guarantee the transport and release of unaltered quercetin at appropriate concentration. One of the most important criteria in drug release is the obtainment of a sustained release that can guarantee a therapeutic efficacy. The present work considered the effect of loading mixtures on quercetin release. A much more sustained release can be obtained by mean of a solvent mixture with a lower ethanol content. This is likely the result of a predominant adsorption mechanism due to the higher water content. Moreover, drug loading obtained with the 50:50 EtOH:H_2O mixture allowed for a quercetin concentration release which matched the concentration found in plasma after oral quercetin administration. These developments were obtained together with a substantial increase in stability of

quercetin. These features revealed a robust DDS with potential antimicrobial effect, further strengthened through the functionalization with the cationic antimicrobial polypeptide PLL.

4.Conclusions

In this work different functionalized mesoporous silica nanoparticles, MSN, MSN-NH_2 MSN-TETA, MSN-NH_2-PLL and MSN-TETA-PLL samples were synthesized and characterized by several techniques to prepare a new DDS for quercetin. Due to the poor solubility of quercetin in water, an ethanol-water mixture was used for loading quercetin into MSNs. Two different EtOH:H_2O ratios (80:20 and 50:50) were investigated. While loading was favored by the solvent with the higher content of ethanol, the best release performance was obtained using an EtOH:H_2O 50:50 mixture for all functionalized MSNs. These results clearly demonstrate that the choice of the solvent used in the loading step of a poorly water-soluble drug is a key factor in the release performance. Lowering ethanol content favors the physical adsorption on functionalized MSN nanoparticles significantly with respect to the impregnation process. The physical adsorption of quercetin at the surface functional groups consequently slows down the release as demonstrated by the significant decrease of the kinetic constants. The PLL grafted MSNs showed slightly higher release kinetics, however the released amounts of quercetin were always in the range 0.2 - 3 µg/mL, that is the concentration range found in plasma after quercetin supplements assumption. Remarkably, immobilization on PLL grafted functionalized MSNs preserved quercetin stability avoiding its oxidation up to 6 h.

In summary, we demonstrated that for quercetin the composition of the solvent mixture used in the loading step allows to obtain a better performance of the release particularly in terms of kinetic constant and amount of released drug. The results of this work suggest that when dealing with poorly water-soluble drugs the optimization of solvent mixture composition should be considered to maximize the DDS loading and release performances. Here, the designed DDS seems to guarantee the transport, the protection, and the release of native quercetin at the optimal concentration.

Acknowledgements

Financial supports from, FIR 2020, Fondazione di Sardegna (FdS, F72F20000230007), and Regione Autonoma della Sardegna L.R. 7 RASSR79857, and RASSR81788 (CUP: J81G17000150002) are gratefully acknowledged. C.C. thanks MIUR (PON-AIM Azione I.2, DD 407- 27.02.2018, AIM1890410-2) for funding.

References

(1) Nordström, R.; Malmsten, M. Delivery Systems for Antimicrobial Peptides. *Adv. Colloid Interface Sci.* **2017**, *242*, 17–34. https://doi.org/10.1016/j.cis.2017.01.005.

(2) Malekkhaiat Häffner, S.; Malmsten, M. Interplay between Amphiphilic Peptides and Nanoparticles for Selective Membrane Destabilization and Antimicrobial Effects. *Curr. Opin. Colloid Interface Sci.* **2019**, *44*, 59–71. https://doi.org/10.1016/j.cocis.2019.09.004.

(3) Nalwa, H. S. A Special Issue on Reviews in Nanomedicine, Drug Delivery and Vaccine Development. *J. Biomed. Nanotechnol.* **2014**, *10* (9), 1635–1640. https://doi.org/10.1166/jbn.2014.2033.

(4) Aslan, S.; Deneufchatel, M.; Hashmi, S.; Li, N.; Pfefferle, L. D.; Elimelech, M.; Pauthe, E.; Van Tassel, P. R. Carbon Nanotube-Based Antimicrobial Biomaterials Formed via Layer-by-Layer Assembly with Polypeptides. *J. Colloid Interface Sci.* **2012**, *388* (1), 268–273. https://doi.org/10.1016/j.jcis.2012.08.025.

(5) Abeer, M. M.; Rewatkar, P.; Qu, Z.; Talekar, M.; Kleitz, F.; Schmid, R.; Lindén, M.; Kumeria, T.; Popat, A. Silica Nanoparticles: A Promising Platform for Enhanced Oral Delivery of Macromolecules. *J. Control. Release* **2020**, *326* (July), 544–555. https://doi.org/10.1016/j.jconrel.2020.07.021.

(6) Cho, H.; Lai, T. C.; Tomoda, K.; Kwon, G. S. Polymeric Micelles for Multi-Drug Delivery in

Cancer. *AAPS PharmSciTech* **2014**, *16* (1), 10–20. https://doi.org/10.1208/s12249-014-0251-3.

(7) Hallaj-Nezhadi, S.; Hassan, M. Nanoliposome-Based Antibacterial Drug Delivery. *Drug Deliv.* **2015**, *22* (5), 581–589. https://doi.org/10.3109/10717544.2013.863409.

(8) Nizamov, T. R.; Garanina, A. S.; Grebennikov, I. S.; Zhironkina, O. A.; Strelkova, O. S.; Alieva, I. B.; Kireev, I. I.; Abakumov, M. A.; Savchenko, A. G.; Majouga, A. G. Effect of Iron Oxide Nanoparticle Shape on Doxorubicin Drug Delivery Toward LNCaP and PC-3 Cell Lines. *Bionanoscience* **2018**, *8* (1), 394–406. https://doi.org/10.1007/s12668-018-0502-y.

(9) Mas, N.; Galiana, I.; Mondragõn, L.; Aznar, E.; Climent, E.; Cabedo, N.; Sancenõn, F.; Murguía, J. R.; Martínez-Máñez, R.; Marcos, M. D.; Amorõs, P. Enhanced Efficacy and Broadening of Antibacterial Action of Drugs via the Use of Capped Mesoporous Nanoparticles. *Chem. - A Eur. J.* **2013**, *19* (34), 11167–11171. https://doi.org/10.1002/chem.201302170.

(10) Braun, K.; Pochert, A.; Lindén, M.; Davoudi, M.; Schmidtchen, A.; Nordström, R.; Malmsten, M. Membrane Interactions of Mesoporous Silica Nanoparticles as Carriers of Antimicrobial Peptides. *J. Colloid Interface Sci.* **2016**, *475*, 161–170. https://doi.org/10.1016/j.jcis.2016.05.002.

(11) Vallet-Regí, M.; Colilla, M.; Izquierdo-Barba, I.; Manzano, M. Mesoporous Silica Nanoparticles for Drug Delivery: Current Insights. *Molecules* **2018**, *23* (1), 1–19. https://doi.org/10.3390/molecules23010047.

(12) Salis, A.; Fanti, M.; Medda, L.; Nairi, V.; Cugia, F.; Piludu, M.; Sogos, V.; Monduzzi, M. Mesoporous Silica Nanoparticles Functionalized with Hyaluronic Acid and Chitosan Biopolymers. Effect of Functionalization on Cell Internalization. *ACS Biomater. Sci. Eng.*

2016, *2* (5), 741–751. https://doi.org/10.1021/acsbiomaterials.5b00502.

(13) Nairi, V.; Magnolia, S.; Piludu, M.; Nieddu, M.; Caria, C. A.; Sogos, V.; Vallet-Regì, M.; Monduzzi, M.; Salis, A. Mesoporous Silica Nanoparticles Functionalized with Hyaluronic Acid. Effect of the Biopolymer Chain Length on Cell Internalization. *Colloids Surfaces B Biointerfaces* **2018**, *168*, 50–59. https://doi.org/10.1016/j.colsurfb.2018.02.019.

(14) Nairi, V.; Medda, L.; Monduzzi, M.; Salis, A. Adsorption and Release of Ampicillin Antibiotic from Ordered Mesoporous Silica. *J. Colloid Interface Sci.* **2017**, *497*, 217–225. https://doi.org/10.1016/j.jcis.2017.03.021.

(15) Magner, E. Immobilisation of Enzymes on Mesoporous Silicate Materials. *Chem. Soc. Rev.* **2013**, *42* (15), 6213–6222. https://doi.org/10.1039/c2cs35450k.

(16) Niculescu, V. C. Mesoporous Silica Nanoparticles for Bio-Applications. *Front. Mater.* **2020**, *7* (February), 1–14. https://doi.org/10.3389/fmats.2020.00036.

(17) Sábio, R. M.; Meneguin, A. B.; Martins dos Santos, A.; Monteiro, A. S.; Chorilli, M. Exploiting Mesoporous Silica Nanoparticles as Versatile Drug Carriers for Several Routes of Administration. *Microporous Mesoporous Mater.* **2021**, *312* (November 2020). https://doi.org/10.1016/j.micromeso.2020.110774.

(18) Day, C. M.; Sweetman, M. J.; Song, Y.; Plush, S. E.; Garg, S. Applied Sciences Functionalized Mesoporous Silica Nanoparticles as Delivery Systems for Doxorubicin : Drug Loading and Release. **2021**, 14–16.

(19) Mamaeva, V.; Sahlgren, C.; Lindén, M. Mesoporous Silica Nanoparticles in Medicine—Recent Advances. *Adv. Drug Deliv. Rev.* **2013**, *65* (5), 689–702. https://doi.org/10.1016/j.addr.2012.07.018.

(20) Rosenholm, J. M.; Sahlgren, C.; Lindén, M. Towards Multifunctional, Targeted Drug

Delivery Systems Using Mesoporous Silica Nanoparticles – Opportunities & Challenges. *Nanoscale* **2010**, *2* (10), 1870. https://doi.org/10.1039/c0nr00156b.

(21) Carvalho, G. C.; Sábio, R. M.; de Cássia Ribeiro, T.; Monteiro, A. S.; Pereira, D. V.; Ribeiro, S. J. L.; Chorilli, M. Highlights in Mesoporous Silica Nanoparticles as a Multifunctional Controlled Drug Delivery Nanoplatform for Infectious Diseases Treatment. *Pharm. Res.* **2020**, *37* (10). https://doi.org/10.1007/s11095-020-02917-6.

(22) Lin, C. Y.; Yang, C. M.; Lindén, M. Influence of Serum Concentration and Surface Functionalization on the Protein Adsorption to Mesoporous Silica Nanoparticles. *RSC Adv.* **2019**, *9* (58), 33912–33921. https://doi.org/10.1039/c9ra05585a.

(23) Patil, N. A.; Kandasubramanian, B. Functionalized Polylysine Biomaterials for Advanced Medical Applications: A Review. *Eur. Polym. J.* **2021**, *146* (November 2020), 110248. https://doi.org/10.1016/j.eurpolymj.2020.110248.

(24) Zheng, M.; Pan, M.; Zhang, W.; Lin, H.; Wu, S.; Lu, C.; Tang, S.; Liu, D.; Cai, J. Poly(α-L-Lysine)-Based Nanomaterials for Versatile Biomedical Applications: Current Advances and Perspectives. *Bioact. Mater.* **2021**, *6* (7), 1878–1909. https://doi.org/10.1016/j.bioactmat.2020.12.001.

(25) Shih, I.-; Van, Y.-; Shen, M.-. Biomedical Applications of Chemically and Microbiologically Synthesized Poly(Glutamic Acid) and Poly(Lysine). *Mini-Reviews Med. Chem.* **2005**, *4* (2), 179–188. https://doi.org/10.2174/1389557043487420.

(26) Manouchehri, S.; Zarrintaj, P.; Saeb, M. R.; Ramsey, J. D. Advanced Delivery Systems Based on Lysine or Lysine Polymers. *Mol. Pharm.* **2021**, *18* (10), 3652–3670. https://doi.org/10.1021/acs.molpharmaceut.1c00474.

(27) Mohammed, S. A. A.; Khan, R. A.; El-readi, M. Z.; Emwas, A. H.; Sioud, S.; Poulson, B. G.; Jaremko, M.; Eldeeb, H. M.; Al-omar, M. S.; Mohammed, H. A. Suaeda Vermiculata

Aqueous-ethanolic Extract-based Mitigation of Ccl4-induced Hepatotoxicity in Rats, and Hepg-2 and Hepg-2/Adr Cell-lines-based Cytotoxicity Evaluations. *Plants* **2020**, *9* (10), 1–26. https://doi.org/10.3390/plants9101291.

(28) El-Saber Batiha, G.; Beshbishy, A. M.; Ikram, M.; Mulla, Z. S.; Abd El-Hack, M. E.; Taha, A. E.; Algammal, A. M.; Ali Elewa, Y. H. The Pharmacological Activity, Biochemical Properties, and Pharmacokinetics of the Major Natural Polyphenolic Flavonoid: Quercetin. *Foods* **2020**, *9* (3). https://doi.org/10.3390/foods9030374.

(29) Sato, S.; Mukai, Y. Modulation of Chronic Inflammation by Quercetin: The Beneficial Effects on Obesity. *J. Inflamm. Res.* **2020**, *13*, 421–431. https://doi.org/10.2147/JIR.S228361.

(30) Vafadar, A.; Shabaninejad, Z.; Movahedpour, A.; Fallahi, F.; Taghavipour, M.; Ghasemi, Y.; Akbari, M.; Shafiee, A.; Hajighadimi, S.; Moradizarmehri, S.; Razi, E.; Savardashtaki, A.; Mirzaei, H. Quercetin and Cancer: New Insights into Its Therapeutic Effects on Ovarian Cancer Cells. *Cell Biosci.* **2020**, *10* (1), 1–17. https://doi.org/10.1186/s13578-020-00397-0.

(31) Xu, D.; Hu, M. J.; Wang, Y. Q.; Cui, Y. L. Antioxidant Activities of Quercetin and Its Complexes for Medicinal Application. *Molecules* **2019**, *24* (6). https://doi.org/10.3390/molecules24061123.

(32) Jaisinghani, R. N. Antibacterial Properties of Quercetin. *Microbiol. Res. (Pavia).* **2017**, *8* (1). https://doi.org/10.4081/mr.2017.6877.

(33) Badshah, S. L.; Faisal, S.; Muhammad, A.; Poulson, B. G.; Emwas, A. H.; Jaremko, M. Antiviral Activities of Flavonoids. *Biomed. Pharmacother.* **2021**, *140* (March), 111596. https://doi.org/10.1016/j.biopha.2021.111596.

(34) Yang, D.; Wang, T.; Long, M.; Li, P. Quercetin: Its Main Pharmacological Activity and Potential Application in Clinical Medicine. *Oxid. Med. Cell. Longev.* **2020**, *2020*.

https://doi.org/10.1155/2020/8825387.

(35) Wang, Y.; Tao, B.; Wan, Y.; Sun, Y.; Wang, L.; Sun, J.; Li, C. Drug Delivery Based Pharmacological Enhancement and Current Insights of Quercetin with Therapeutic Potential against Oral Diseases. *Biomed. Pharmacother.* **2020**, *128* (May), 110372. https://doi.org/10.1016/j.biopha.2020.110372.

(36) Wang, S.; Yao, J.; Zhou, B.; Yang, J.; Chaudry, M. T.; Wang, M.; Xiao, F.; Li, Y.; Yin, W. Bacteriostatic Effect of Quercetin as an Antibiotic Alternative in Vivo and Its Antibacterial Mechanism in Vitro. *J. Food Prot.* **2018**, *81* (1), 68–78. https://doi.org/10.4315/0362-028X.JFP-17-214.

(37) Gao, L.; Liu, G.; Wang, X.; Liu, F.; Xu, Y.; Ma, J. Preparation of a Chemically Stable Quercetin Formulation Using Nanosuspension Technology. *Int. J. Pharm.* **2011**, *404* (1–2), 231–237. https://doi.org/10.1016/j.ijpharm.2010.11.009.

(38) E.A. AbouAitah, K.; A. Farghali, A. Mesoporous Silica Materials in Drug Delivery System: PH/Glutathione- Responsive Release of Poorly Water-Soluble Pro-Drug Quercetin from Two and Three-Dimensional Pore-Structure Nanoparticles. *J. Nanomed. Nanotechnol.* **2016**, *07* (02). https://doi.org/10.4172/2157-7439.1000360.

(39) Scalia, S.; Mezzena, M. Incorporation of Quercetin in Lipid Microparticles: Effect on Photo- and Chemical-Stability. *J. Pharm. Biomed. Anal.* **2009**, *49* (1), 90–94. https://doi.org/10.1016/j.jpba.2008.10.011.

(40) Berlier, G.; Gastaldi, L.; Ugazio, E.; Miletto, I.; Iliade, P.; Sapino, S. Stabilization of Quercetin Flavonoid in MCM-41 Mesoporous Silica: Positive Effect of Surface Functionalization. *J. Colloid Interface Sci.* **2013**, *393* (1), 109–118. https://doi.org/10.1016/j.jcis.2012.10.073.

(41) Sarkar, A.; Ghosh, S.; Chowdhury, S.; Pandey, B.; Sil, P. C. Targeted Delivery of Quercetin

Loaded Mesoporous Silica Nanoparticles to the Breast Cancer Cells. *Biochim. Biophys. Acta - Gen. Subj.* **2016**, *1860* (10), 2065–2075. https://doi.org/10.1016/j.bbagen.2016.07.001.

(42) Pinheiro, R. G. R.; Pinheiro, M.; Neves, A. R. Nanotechnology Innovations to Enhance the Therapeutic Efficacy of Quercetin. *Nanomaterials* **2021**, *11* (10), 1–26. https://doi.org/10.3390/nano11102658.

(43) Khan, M. A.; Zhou, C.; Zheng, P.; Zhao, M.; Liang, L. Improving Physicochemical Stability of Quercetin-Loaded Hollow Zein Particles with Chitosan/Pectin Complex Coating. *Antioxidants* **2021**, *10* (9). https://doi.org/10.3390/antiox10091476.

(44) He, Y.; Liang, S.; Long, M.; Xu, H. Mesoporous Silica Nanoparticles as Potential Carriers for Enhanced Drug Solubility of Paclitaxel. *Mater. Sci. Eng. C* **2017**, *78*, 12–17. https://doi.org/10.1016/j.msec.2017.04.049.

(45) García-Casas, I.; Crampon, C.; Montes, A.; Pereyra, C.; Martínez de la Ossa, E. J.; Badens, E. Supercritical CO2 Impregnation of Silica Microparticles with Quercetin. *J. Supercrit. Fluids* **2019**, *143* (April 2018), 157–161. https://doi.org/10.1016/j.supflu.2018.07.019.

(46) Abouaitah, K.; Lojkowski, W. Delivery of Natural Agents by Means of Mesoporous Silica Nanospheres as a Promising Anticancer Strategy. *Pharmaceutics* **2021**, *13* (2), 1–53. https://doi.org/10.3390/pharmaceutics13020143.

(47) Liang, Q.; Sun, X.; Raza, H.; Aslam Khan, M.; Ma, H.; Ren, X. Fabrication and Characterization of Quercetin Loaded Casein Phosphopeptides-Chitosan Composite Nanoparticles by Ultrasound Treatment: Factor Optimization, Formation Mechanism, Physicochemical Stability and Antioxidant Activity. *Ultrason. Sonochem.* **2021**, *80*, 105830. https://doi.org/10.1016/j.ultsonch.2021.105830.

(48) Ghanimati, M.; Jabbari, M.; Farajtabar, A.; Nabavi-Amri, S. A. Adsorption Kinetics and Isotherms of Bioactive Antioxidant Quercetin onto Amino-Functionalized Silica

Nanoparticles in Aqueous Ethanol Solutions. *New J. Chem.* **2017**, *41* (16), 8451–8458. https://doi.org/10.1039/c7nj01489a.

(49) Rubini, K.; Boanini, E.; Menichetti, A.; Bonvicini, F.; Gentilomi, G. A.; Montalti, M.; Bigi, A. Quercetin Loaded Gelatin Films with Modulated Release and Tailored Anti-Oxidant, Mechanical and Swelling Properties. *Food Hydrocoll.* **2020**, *109* (March), 106089. https://doi.org/10.1016/j.foodhyd.2020.106089.

(50) Sapino, S.; Ugazio, E.; Gastaldi, L.; Miletto, I.; Berlier, G.; Zonari, D.; Oliaro-Bosso, S. Mesoporous Silica as Topical Nanocarriers for Quercetin: Characterization and in Vitro Studies. *Eur. J. Pharm. Biopharm.* **2015**, *89*, 116–125. https://doi.org/10.1016/j.ejpb.2014.11.022.

(51) Zaharudin, N. S.; Mohamed Isa, E. D.; Ahmad, H.; Abdul Rahman, M. B.; Jumbri, K. Functionalized Mesoporous Silica Nanoparticles Templated by Pyridinium Ionic Liquid for Hydrophilic and Hydrophobic Drug Release Application. *J. Saudi Chem. Soc.* **2020**, *24* (3), 289–302. https://doi.org/10.1016/j.jscs.2020.01.003.

(52) Kazakova, O. A.; Gun'ko, V. M.; Lipkovskaya, N. A.; Voronin, E. F.; Pogorelyi, V. K. Interaction of Quercetin with Highly Dispersed Silica in Aqueous Suspensions. *Colloid J.* **2002**, *64* (4), 412–418. https://doi.org/10.1023/A:1016807717891.

(53) Islami, M.; Zarrabi, A.; Tada, S.; Kawamoto, M.; Isoshima, T.; Ito, Y. Controlled Quercetin Release from High-Capacity-Loading Hyperbranched Polyglycerol-Functionalized Graphene Oxide. *Int. J. Nanomedicine* **2018**, *13*, 6059–6071. https://doi.org/10.2147/IJN.S178374.

(54) Lee, D.-H.; Sim, G.-S.; Kim, J.-H.; Lee, G.-S.; Pyo, H.-B.; Lee, B.-C. Preparation and Characterization of Quercetin-Loaded Polymethyl Methacrylate Microcapsules Using a Polyol-in-Oil-in-Polyol Emulsion Solvent Evaporation Method. *J. Pharm. Pharmacol.* **2010**, *59* (12), 1611–1620. https://doi.org/10.1211/jpp.59.12.0002.

(55) Steri, D.; Monduzzi, M.; Salis, A. Ionic Strength Affects Lysozyme Adsorption and Release from SBA-15 Mesoporous Silica. *Microporous Mesoporous Mater.* **2013**, *170*, 164–172. https://doi.org/10.1016/j.micromeso.2012.12.002.

(56) Batys, P.; Morga, M.; Bonarek, P.; Sammalkorpi, M. PH-Induced Changes in Polypeptide Conformation: Force-Field Comparison with Experimental Validation. *J. Phys. Chem. B* **2020**, *124* (14), 2961–2972. https://doi.org/10.1021/acs.jpcb.0c01475.

(57) Lee, N.-K.; Park, S. S.; Ha, C.-S. PH-Sensitive Drug Delivery System Based on Mesoporous Silica Modified with Poly-L-Lysine (PLL) as a Gatekeeper. *J. Nanosci. Nanotechnol.* **2020**, *20* (11), 6925–6934. https://doi.org/10.1166/jnn.2020.18821.

(58) Gonçalves, J. L. M.; Lopes, A. B. C.; Baleizão, C.; Farinha, J. P. S. Mesoporous Silica Nanoparticles Modified inside and out for on:Off Ph-Modulated Cargo Release. *Pharmaceutics* **2021**, *13* (5). https://doi.org/10.3390/pharmaceutics13050716.

(59) Beck, J. S.; Vartuli, J. C.; Roth, W. J.; Leonowicz, M. E.; Kresge, C. T.; Schmitt, K. D.; Chu, C. T. W.; Olson, D. H.; Sheppard, E. W.; McCullen, S. B.; Higgins, J. B.; Schlenker, J. L. A New Family of Mesoporous Molecular Sieves Prepared with Liquid Crystal Templates. *J. Am. Chem. Soc.* **1992**, *114* (27), 10834–10843. https://doi.org/10.1021/ja00053a020.

(60) Maleki, A.; Kettiger, H.; Schoubben, A.; Rosenholm, J. M.; Ambrogi, V.; Hamidi, M. Mesoporous Silica Materials: From Physico-Chemical Properties to Enhanced Dissolution of Poorly Water-Soluble Drugs. *J. Control. Release* **2017**, *262* (July), 329–347. https://doi.org/10.1016/j.jconrel.2017.07.047.

(61) Trendafilova, I.; Szegedi, A.; Mihály, J.; Momekov, G.; Lihareva, N.; Popova, M. Preparation of Efficient Quercetin Delivery System on Zn-Modified Mesoporous SBA-15 Silica Carrier. *Mater. Sci. Eng. C* **2017**, *73*, 285–292. https://doi.org/10.1016/j.msec.2016.12.063.

(62) Hudson, S. P.; Padera, R. F.; Langer, R.; Kohane, D. S. The Biocompatibility of Mesoporous Silicates. *Biomaterials* **2008**, *29* (30), 4045–4055. https://doi.org/10.1016/j.biomaterials.2008.07.007.

(63) Kohane, D. S.; Langer, R. Biocompatibility and Drug Delivery Systems. *Chem. Sci.* **2010**, *1* (4), 441–446. https://doi.org/10.1039/c0sc00203h.

(64) Naahidi, S.; Jafari, M.; Edalat, F.; Raymond, K.; Khademhosseini, A.; Chen, P. Biocompatibility of Engineered Nanoparticles for Drug Delivery. *J. Control. Release* **2013**, *166* (2), 182–194. https://doi.org/10.1016/j.jconrel.2012.12.013.

(65) Chen, L.; Liu, J.; Zhang, Y.; Zhang, G.; Kang, Y.; Chen, A.; Feng, X.; Shao, L. The Toxicity of Silica Nanoparticles to the Immune System. *Nanomedicine* **2018**, *13* (15), 1939–1962. https://doi.org/10.2217/nnm-2018-0076.

(66) Yang, C.; Shi, Z.; Feng, C.; Li, R.; Luo, S.; Li, X.; Ruan, L. An Adjustable PH-Responsive Drug Delivery System Based on Self-Assembly Polypeptide-Modified Mesoporous Silica. *Macromol. Biosci.* **2020**, *20* (6), 1–10. https://doi.org/10.1002/mabi.202000034.

(67) Li, Z.; Moalin, M.; Zhang, M.; Vervoort, L.; Hursel, E.; Mommers, A.; Haenen, G. R. M. M. The Flow of the Redox Energy in Quercetin during Its Antioxidant Activity in Water. *Int. J. Mol. Sci.* **2020**, *21* (17), 1–16. https://doi.org/10.3390/ijms21176015.

(68) Chebotarev, A. N.; Snigur, D. V. Study of the Acid-Base Properties of Quercetin in Aqueous Solutions by Color Measurements. *J. Anal. Chem.* **2015**, *70* (1), 55–59. https://doi.org/10.1134/S1061934815010062.

(69) Jovanovic, S. V.; Steenken, S.; Tosic, M.; Marjanovic, B.; Simic, M. G. Flavonoids as Antioxidants. *J. Am. Chem. Soc.* **1994**, *116* (11), 4846–4851. https://doi.org/10.1021/ja00090a032.

(70) Álvarez-Diduk, R.; Ramírez-Silva, M. T.; Galano, A.; Merkoçi, A. Deprotonation Mechanism and Acidity Constants in Aqueous Solution of Flavonols: A Combined Experimental and Theoretical Study. *J. Phys. Chem. B* **2013**, *117* (41), 12347–12359. https://doi.org/10.1021/jp4049617.

(71) Pishnamazi, M.; Hafizi, H.; Pishnamazi, M.; Marjani, A.; Shirazian, S.; Walker, G. M. Controlled Release Evaluation of Paracetamol Loaded Amine Functionalized Mesoporous Silica KCC1 Compared to Microcrystalline Cellulose Based Tablets. *Sci. Rep.* **2021**, *11* (1), 1–11. https://doi.org/10.1038/s41598-020-79983-8.

(72) Dharmayanti, C.; Gillam, T. A.; Klingler-Hoffmann, M.; Albrecht, H.; Blencowe, A. Strategies for the Development of PH-Responsive Synthetic Polypeptides and Polymer-Peptide Hybrids: Recent Advancements. *Polymers (Basel).* **2021**, *13* (4), 1–17. https://doi.org/10.3390/polym13040624.

(73) González, B.; Colilla, M.; Díez, J.; Pedraza, D.; Guembe, M.; Izquierdo-Barba, I.; Vallet-Regí, M. Mesoporous Silica Nanoparticles Decorated with Polycationic Dendrimers for Infection Treatment. *Acta Biomater.* **2018**, *68*, 261–271. https://doi.org/10.1016/j.actbio.2017.12.041.

(74) Vargason, A. M.; Anselmo, A. C.; Mitragotri, S. The Evolution of Commercial Drug Delivery Technologies. *Nat. Biomed. Eng.* **2021**, *5* (9), 951–967. https://doi.org/10.1038/s41551-021-00698-w.

(75) Adepu, S.; Ramakrishna, S. Controlled Drug Delivery Systems: Current Status and Future Directions. *Molecules* **2021**, *26* (19). https://doi.org/10.3390/molecules26195905.

(76) Kaushik, D.; O'Fallon, K.; Clarkson, P. M.; Patrick Dunne, C.; Conca, K. R.; Michniak-Kohn, B. Comparison of Quercetin Pharmacokinetics Following Oral Supplementation in Humans. *J. Food Sci.* **2012**, *77* (11). https://doi.org/10.1111/j.1750-3841.2012.02934.x.

(77) Wang, W.; Sun, C.; Mao, L.; Ma, P.; Liu, F.; Yang, J.; Gao, Y. The Biological Activities, Chemical Stability, Metabolism and Delivery Systems of Quercetin: A Review. *Trends Food Sci. Technol.* **2016**, *56*, 21–38. https://doi.org/10.1016/j.tifs.2016.07.004.

(78) Moon, Y.J., Wang, L., DiCenzo, R. and Morris, M. E. Quercetin Pharmacokinetics in Humans. *Biopharm. Drug Dispos.* **2008**, *29* (3), 205–217. https://doi.org/doi.org/10.1002/bdd.605.

(79) Lei, R.; Xu, X.; Yu, F.; Li, N.; Liu, H. W.; Li, K. A Method to Determine Quercetin by Enhanced Luminol Electrogenerated Chemiluminescence (ECL) and Quercetin Autoxidation. *Talanta* **2008**, *75* (4), 1068–1074. https://doi.org/10.1016/j.talanta.2008.01.010.

(80) Zenkevich, I. G.; Eshchenko, A. Y.; Makarova, S. V.; Vitenberg, A. G.; Dobryakov, Y. G.; Utsal, V. A. Identification of the Products of Oxidation of Quercetin by Air Oxygen at Ambient Temperature. *Molecules* **2007**, *12* (3), 654–672. https://doi.org/10.3390/12030654.

(81) Ravichandran, R.; Rajendran, M.; Devapiriam, D. Antioxidant Study of Quercetin and Their Metal Complex and Determination of Stability Constant by Spectrophotometry Method. *Food Chem.* **2014**, *146*, 472–478. https://doi.org/10.1016/j.foodchem.2013.09.080.

(82) Biler, M.; Biedermann, D.; Valentová, K.; Křen, V.; Kubala, M. Quercetin and Its Analogues: Optical and Acido-Basic Properties. *Phys. Chem. Chem. Phys.* **2017**, *19* (39), 26870–26879. https://doi.org/10.1039/c7cp03845c.

(83) Jurasekova, Z.; Domingo, C.; Garcia-Ramos, J. V.; Sanchez-Cortes, S. Effect of PH on the Chemical Modification of Quercetin and Structurally Related Flavonoids Characterized by Optical (UV-Visible and Raman) Spectroscopy. *Phys. Chem. Chem. Phys.* **2014**, *16* (25), 12802–12811. https://doi.org/10.1039/c4cp00864b.

(84) Jurasekova, Z.; Torreggiani, A.; Tamba, M.; Sanchez-Cortes, S.; Garcia-Ramos, J. V. Raman and Surface-Enhanced Raman Scattering (SERS) Investigation of the Quercetin Interaction

with Metals: Evidence of Structural Changing Processes in Aqueous Solution and on Metal Nanoparticles. *J. Mol. Struct.* **2009**, *918* (1–3), 129–137. https://doi.org/10.1016/j.molstruc.2008.07.025.

(85) Kellil, A.; Grigorakis, S.; Loupassaki, S.; Makris, D. P. Empirical Kinetic Modelling and Mechanisms of Quercetin Thermal Degradation in Aqueous Model Systems: Effect of PH and Addition of Antioxidants. *Appl. Sci.* **2021**, *11* (6). https://doi.org/10.3390/app11062579.

(86) Golonka, I.; Wilk, S.; Musiał, W. The Influence of UV Radiation on the Degradation of Pharmaceutical Formulations Containing Quercetin. *Molecules* **2020**, *25* (22). https://doi.org/10.3390/molecules25225454.

(87) Mocek, B. M.; Richardson, P. J.; Breweries, C.; West, L. A. Kinetics and Mechanism of Quercetin Oxidation. **1972**, *78*.